Supplementary Information

SABER amplifies FISH: enhanced multiplexed imaging of RNA and DNA in cells and tissues

Jocelyn Y. Kishi[1,2,5] Sylvain W. Lapan[3,5] Brian J. Beliveau[1,2,4,5*] Emma R. West[3,5] Allen Zhu[1,2] Hiroshi M. Sasaki[1,2] Sinem K. Saka[1,2] Yu Wang[1,2] Constance L. Cepko[3*] Peng Yin[1,2*]

Wyss Institute for Biologically Inspired Engineering, Harvard University, Boston, MA, USA[1],
Department of Systems Biology, Harvard Medical School, Boston, MA, USA[2],
Department of Genetics, Harvard Medical School, Boston, MA, USA[3],
Present address: Department of Genome Sciences, University of Washington, Seattle, WA, USA[4]
These authors contributed equally[5]

Correspondence*: py@hms.harvard.edu (P.Y.), cepko@genetics.med.harvard.edu (C.L.C.), beliveau@uw.edu (B. J. B.)

Contents

List of Figures

1 Supplemental information for Fig. 1

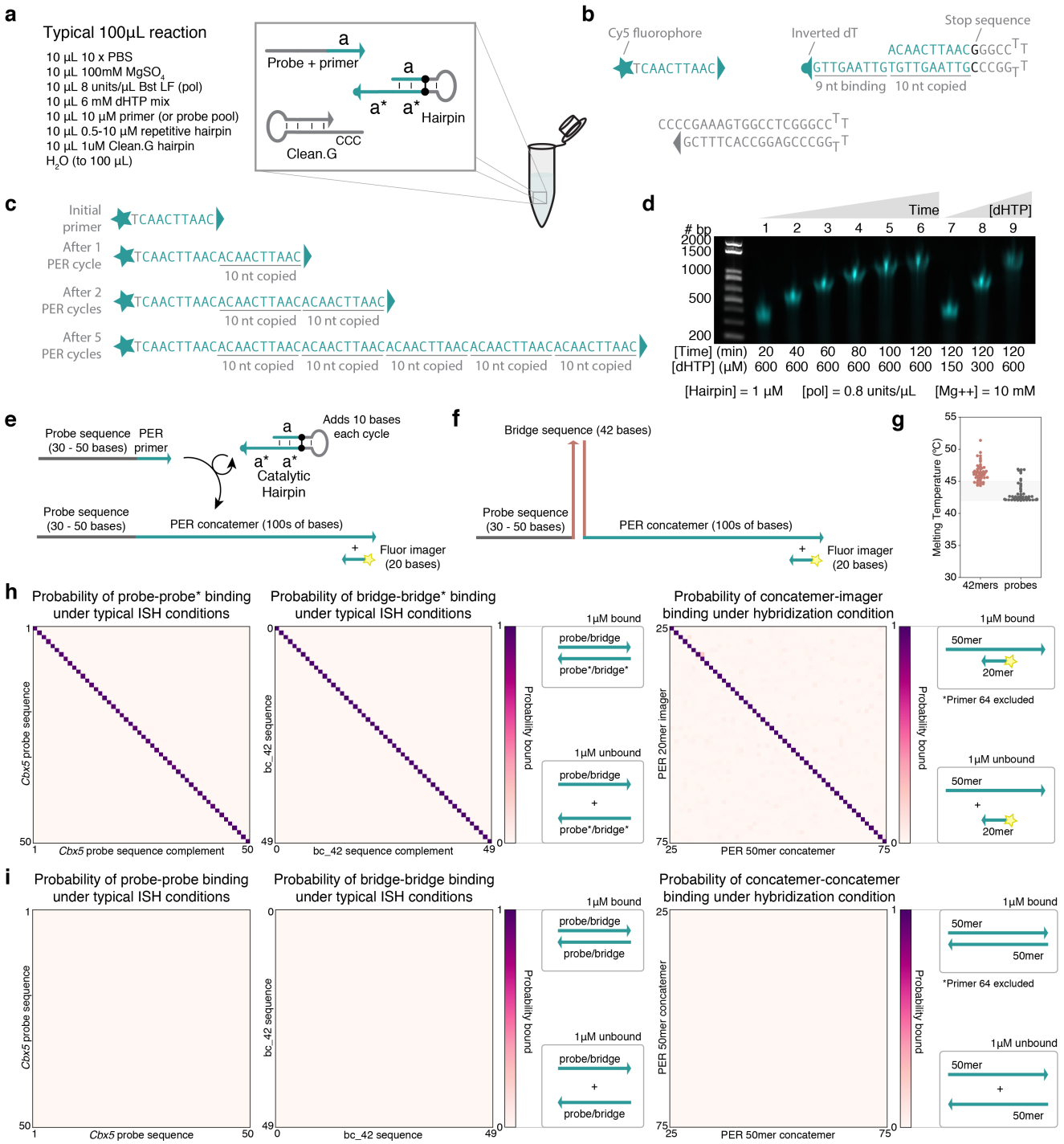

Supplementary Figure 1: **PER design and computational modeling of sequence binding.** **a**, Schematic representation of typical 100 µL PER concatemerization reaction.[1] **b**, Sequence diagrams for oligos used in Fig. 1b. The primer had a Cy5 fluor conjugated on its 5' end and was designed to bind on a 9 nt overhang on the hairpin and copy 10 nt each cycle. **c**, Example concatemer sequences after 0, 1, 2 and 5 PER cycles. **d**, PER concatemer length control by varying incubation time and dHTP (dATP, dTTP, and dCTP) concentration. **e**, Probe sequences are typically computationally designed using the OligMiner pipeline[2] to have 30-50 bases of homology to targets of interest, and they are chemically synthesized with additional short PER primer sequences on their 3' ends. A catalytic hairpin is then used to extend the concatemer sequence *in vitro*. Complementary fluorescent 'fluor' imagers that have 20 bases of homology to the concatemer are typically used for imaging. **f**, Probes may instead be appended with one of 84 available 42mer bridge sequences. The complement of the 42mer bridge sequence can then be appended with a PER primer and concatemerized *in vitro*, followed by co-hybridization with the probe-bridge strands *in situ*. **g**, Melting temperatures of example sets of fifty 42mer bridge and probe sequences calculated with Biopython.[3] The typical FISH temperature range (42°C-45°C) is highlighted. **h**, Orthogonalities of probes, 42mer bridge, and PER sequences. NUPACK[4–6] was used to evaluate the binding probabilities of complementary and orthogonal sequences. The probabilities of the 50 example probes binding to their 50 complementary sequences (left) and of fifty 42mer bridge sequences binding to their 50 complementary sequences (middle) under typical FISH conditions (2×SSCT + 50% formamide at 42°C) shows high likelihood of cognate pairs binding (diagonal of matrix) with little cross-talk between non-cognate sequences. A similar analysis for 50 computationally designed PER primer sequences, analyzing binding probabilities of 50mer concatemers to their complementary 20mers under typical hybridization conditions (1×PBS at 37°C) also shows high levels of orthogonality. **i**, Orthogonality plots calculated with NUPACK[4–6] of the 50 probe, 42mer, and 50mer PER concatemer sequences show that homodimerization and heterodimerization probabilities are negligible under typical hybridization conditions.

2 Supplemental information for Fig. 2

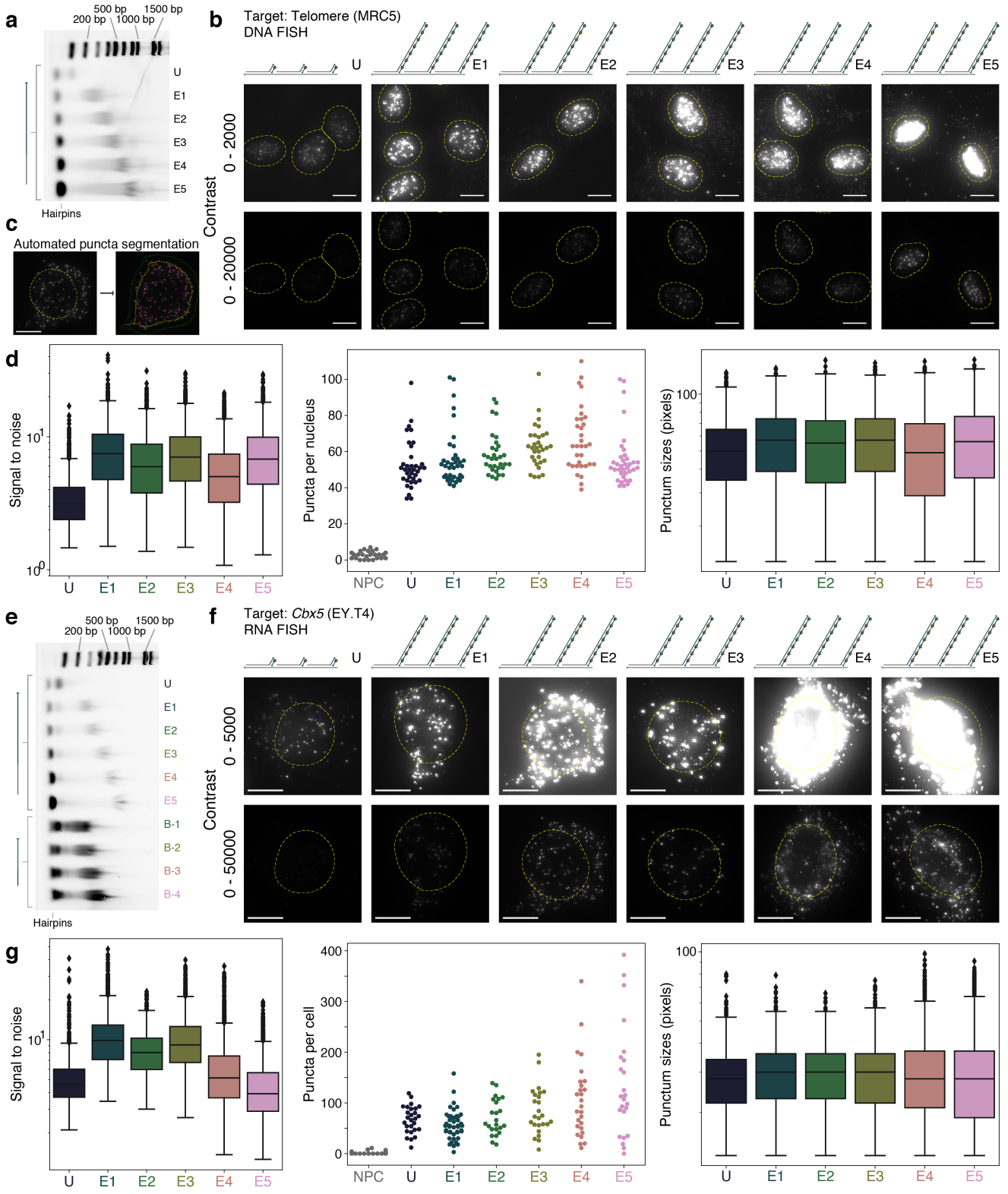

Supplementary Figure 2: **Additional images and quantification of SABER-FISH in cells.** **a**, Gel electrophoresis shows the lengths of the extensions shown in Fig. 2a range from ~250 to 900 nt. **b**, Representative images of all 5 extension length conditions (E1-E5) compared to unextended (U) corresponding to Fig. 2a-b are shown under two contrast settings. **c**, An example microscopy image (left) shown beside an overlay output (right) by the CellProfiler[7] pipeline, which automatically detects cell bodies (green), shrunken cell bodies (yellow), and puncta within these shrunken cell bodies (pink). **d**, Box plots of signal to noise (SNR) values calculated by taking the max intensity value of each punctum and dividing the mean signal level of nuclei masked for identified puncta (left). Swarm plot showing the distribution in puncta counts per nucleus for all conditions (middle). Note that in some cases nuclei have been combined together with 2D segmentation due to proximity. NPC = no probe control condition. Box plots of the focus size (in number of pixels) of identified puncta (right). n(puncta): n(U)=1,895; n(E1)=1,846; n(E2)=1,876; n(E3)=2,011; n(E4)=2,190; n(E5)=2,006. **e**, Gel electrophoresis shows the lengths of the extensions shown in Fig. 2c range from ~250 to 900 nt. Shorter lengths (~250 to 500 nt) were used to characterize one round of branching (see Supplementary Fig. 3b-d). **f**, Representative images of all 5 extension length conditions (E1-E5) compared to unextended (E) corresponding to Fig. 2c-d are shown under two contrast settings. **g**, Box plots of SNR values calculated by taking the max intensity value of each punctum and dividing by the mean signal level of the identified cell body masked for puncta (left). Swarm plot showing the distribution in puncta counts per cell for all conditions (middle). We note that since we did not have a good cell membrane marker for these cells, we used the signal channel as a basis for a watershed-based segmentation algorithm to identify cell bodies. This imperfect segmentation resulted in up to a few cases of cells segmented together per condition as one cell body, particularly in high signal cases. Box plots of the focus size (in number of pixels) of identified puncta (right). n(puncta): n(U)=1,720; n(E1)=1,588; n(E2)=1,649; n(E3)=2,099; n(E4)=2,884; n(E5)=3,279. Scale bars: 10 μm. All box plots show median line and quartiles, with points outside 1.5× the interquartile range shown as outliers.

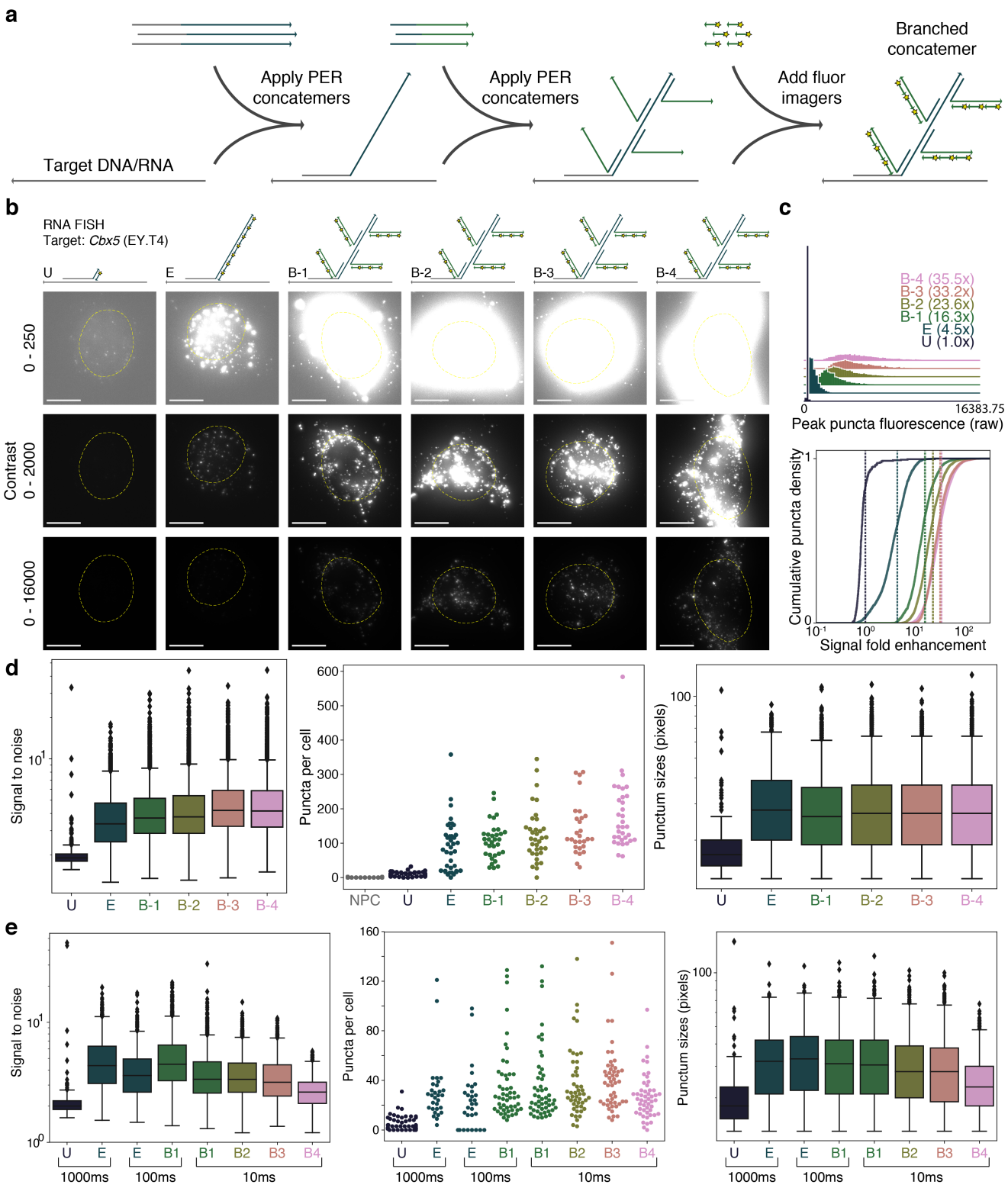
a
Target DNA/RNA
Apply PER concatemers
Apply PER concatemers
Add fluor imagers
Branched concatemer
b
RNA FISH
Target: Cbx5 (EY.T4)
U
E
B-1
B-2
B-3
B-4
0 - 250
Contrast 0 - 2000
0 - 16000
c
B-4 (35.5x)
B-3 (33.2x)
B-2 (23.6x)
B-1 (16.3x)
E (4.5x)
U (1.0x)
0
16383.75
Peak puncta fluorescence (raw)
Cumulative puncta density
Signal fold enhancement
d
Signal to noise
Puncta per cell
NPC
Punctum sizes (pixels)
e
Signal to noise
Puncta per cell
Punctum sizes (pixels)
1000ms
100ms
10ms

Supplementary Figure 3: **Additional branching experiments and quantification.** **a**, Schematic depiction of one round of branching, where a second set of PER concatemers is hybridized to a first set of hybridized concatemer extensions. **b**, Representative images depicting a single round of branching using four different branch sequence lengths (B-1 to B-4, see Supplementary Fig. 2e) compared to single extension (E) and unextended (U) conditions. **c**, Quantification as done in Fig. 2d was used to quantify one round of branching. In total, the longest branch condition (B-4) showed >30 fold amplification over the unextended condition. Mean lines shown on distributions. n(puncta): n(U)=308; n(E)=2,784; n(B-1)=3,542; n(B-2)=4,352; n(B-3)=3,846; n(B-4)=5,916. **d**, Box plots of SNR values calculated by taking the max intensity value of each punctum and dividing by the mean signal level of the identified cell body masked for puncta (left). Swarm plot showing the distribution in puncta counts per cell for all conditions (middle). We note that due to the imaging condition we chose to capture the full distribution dynamic range of the most amplified case (condition B-4) and likely undersampled the unextended probe (condition U) puncta that have signal nearer to background levels. This highlights the technical difficulties of capturing multiple levels of amplification on a single 16-bit scale. Quantification of branched signal (B-1 to B-4) relative to extended but not branched (E) signal is expected to be more accurate than that relative to unextended (U). Box plots of the focus size (in number of pixels) of identified puncta (right). **e**, Box plots of SNR values for the iterative branching experiments (Fig. 2f-g) calculated by taking the max intensity value of each punctum and dividing by the mean signal level of the identified cell body masked for puncta (left). Swarm plot showing the distribution in puncta counts per cell for iterative branching for all conditions (middle). We note that due to the cell density we were unable to segment cells using our previous strategy and instead segmented nuclei using DAPI signal and dilated them by 50 pixels in each direction to define the cell body. This provides a more consistent area considered per cell but underestimates the total number of puncta per cell. Box plots of the focus size (in number of pixels) of identified puncta for iterative branching experiments (right). n(puncta, exposure time): n(U, 1000ms)=262; n(E, 1000ms)=928; n(E, 100ms)=717; n(B1, 100ms)=1,821; n(B1, 10ms)=1,818; n(B2, 10ms)=1,796; n(B3, 10ms)=2,059; n(B4, 10ms)=1,344. Scale bars: 10 μm. All box plots show median line and quartiles, with points outside 1.5× the interquartile range shown as outliers.

3 Supplemental information for Fig. 3

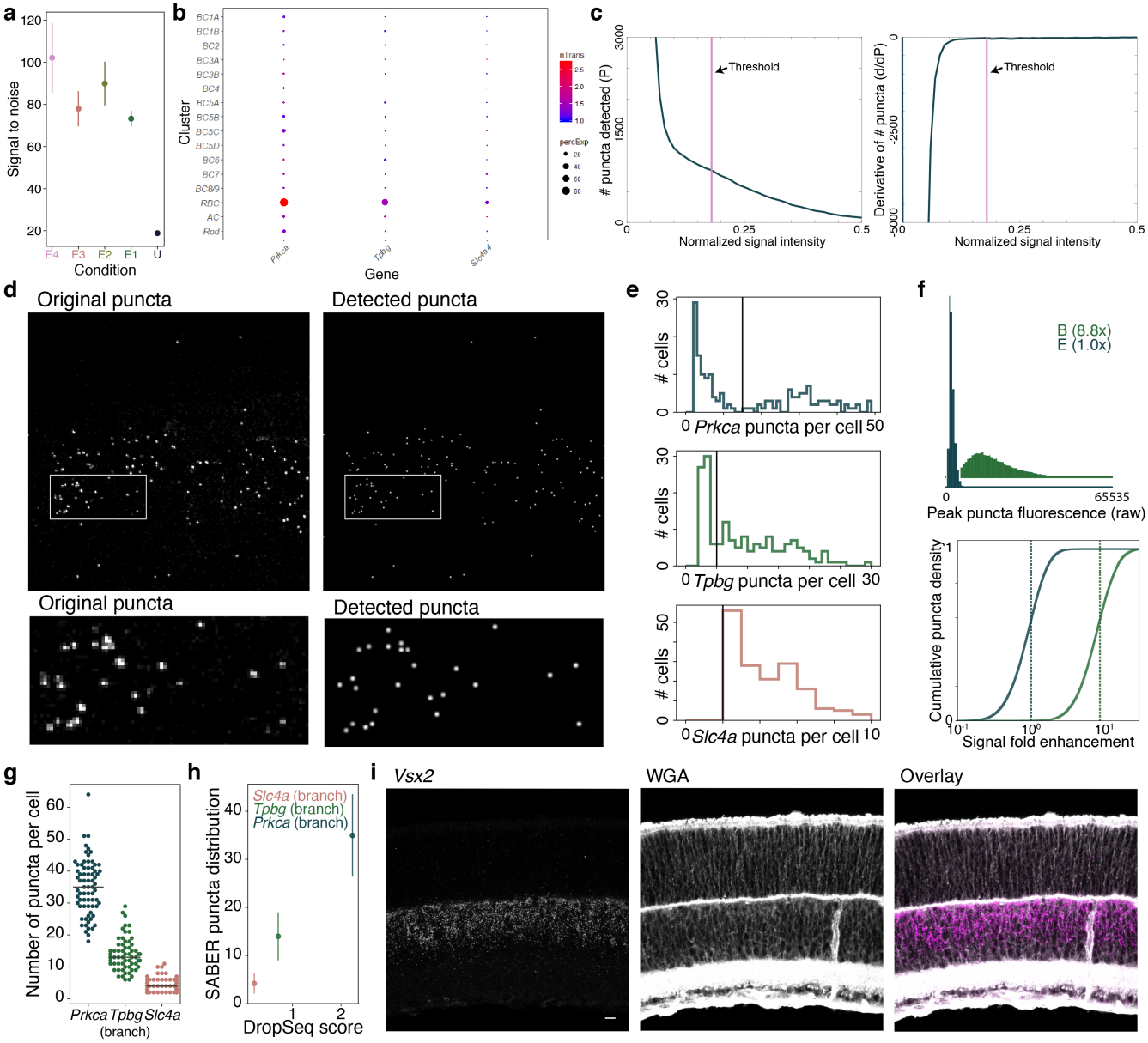

Supplementary Figure 4: **Additional quantification data, segmentation information, and images for SABER-FISH in tissues. a**, Plot of signal to noise (SNR) values calculated for each condition by taking the max intensity value of each puncta and dividing by the mean background. Mean with standard deviation shown for N=4 tissue replicates in each case. **b**, Dot plot of Drop-seq data displaying average transcripts per cell (nTrans) in expressing cells and percent of cells in each cell type cluster with detection of the indicated transcript (percExp) (data from ref[8]). Plot displays all bipolar cell types and amacrine cells (AC) and rods. Note that indicated transcripts are highly enriched in RBCs relative to other bipolar cell types, but may be expressed in subpopulations of ACs and other retinal populations not substantially sampled in the dataset. **c**-**d**, Puncta were detected in 3-D retinal tissue using a custom MATLAB Laplacian of Gaussian (LoG) method. To determine the threshold for each condition, the number of puncta detected across the threshold range were plotted (**c**, left). Generally, we observed a plateau or elbow in the graph where the number of puncta is relatively constant and the derivative graph approaches zero (**c**, right). Choosing a threshold just after the graph plummets to zero generated reliable segmentation results. The pink vertical lines represent the chosen threshold and the resulting detection can be compared to the original SABER image in a 2D projection **(d)**. **e**, Distributions of the number of puncta per cell for each RBC probe. Thresholds for calling positive cells (vertical line) and were chosen to eliminate cells with background levels of transcript. High-abundance transcripts like *Prkca* and *Tpbg* suffer from puncta misassignment to adjacent, negative cells, and thresholding in this way allows us to exclude these cases, yielding a more accurate average value. **f**, Quantification of the increase in signal intensity from branching to *Prkca* detection across three retinal sections. Mean lines shown on distributions. n(puncta): n(E)=35,330; n(B)=29,818. **g**, Quantification of transcripts detected using branched probes. Median lines shown on distributions.. **h**, Quantification of RBC marker transcripts with branching recapitulates relative abundance of transcripts (average number of transcripts per cell) observed from >10,000 single RBCs profiled in the Drop-seq dataset.[8] Standard deviations of SABER puncta per cell are shown. n(cells): n(*Slc4a*)=78; n(*Tpbg*)=65; n(*Prkca*)=71. **i**, Detection of *Vsx2* transcript using a probe pool of 12 extended 47 nt oligos, with a single round of branch amplification. Signal can be compared to *Vsx2* detection in Fig. 5 performed using a set of 40 probes without branch amplification. Retina is P9. Scale bar: 10 μm.

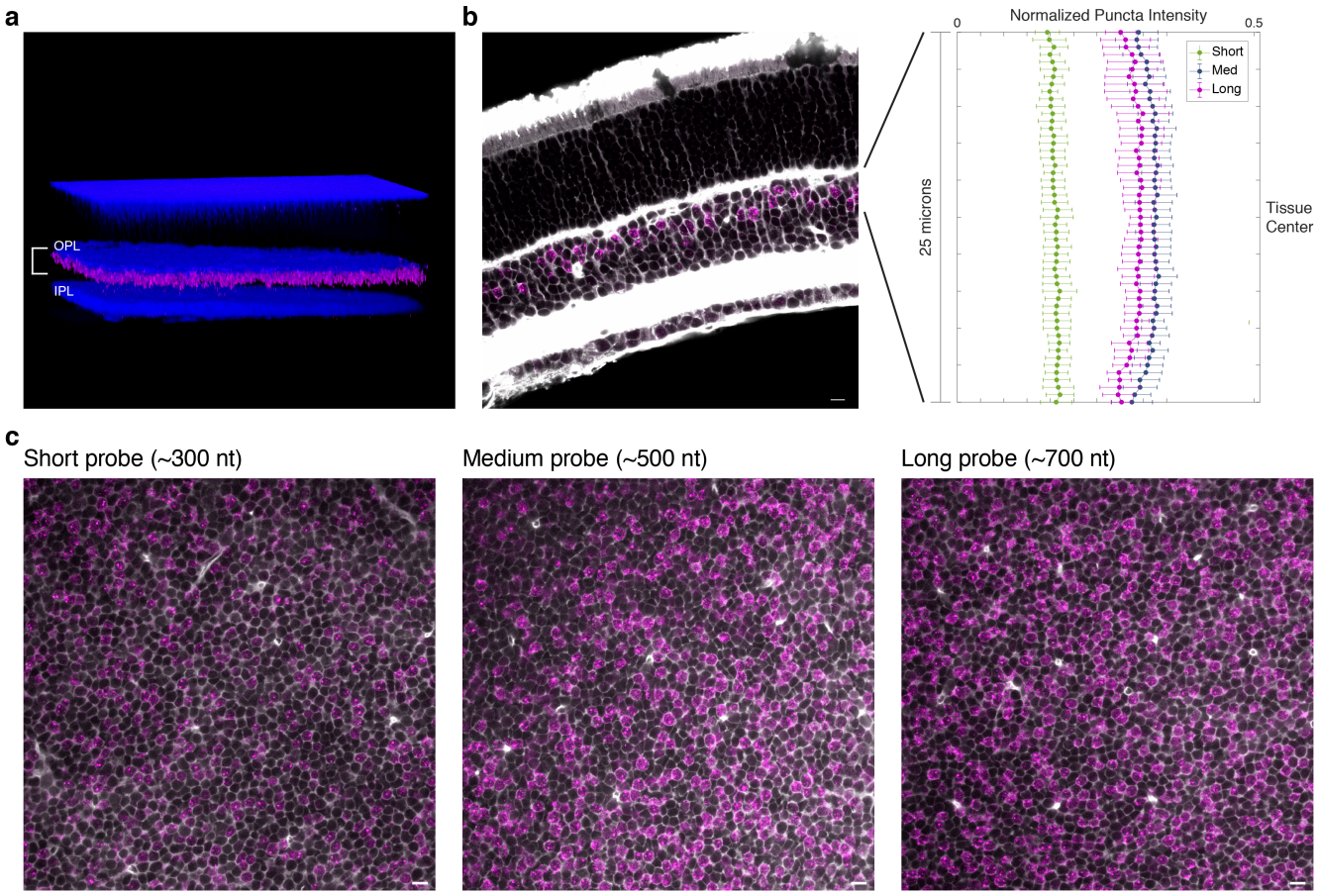

Supplementary Figure 5: **Probe length performance for whole mount retina staining. a**, ImageJ[9] Volume Viewer rendering of whole mount retina stained for *Grik1* expression (magenta) with WGA-labeled landmarks (blue). Bracket shows approximate depth in the Z-dimension imaged for intensity quantification. OPL: Outer Plexiform Layer, IPL: Inner Plexiform Layer. Stack depth: 145 µm. **b**, Transverse cryosection of retina showing *Grik1* RNA expression (left). Quantification of mean FISH signal intensity for probes of three different lengths imaged under identical conditions (right). Sample standard deviation for N=4 regions from separate leaflets for each condition are shown. **c**, Representative images showing *en face* view of *Grik1* expression in the inner nuclear layer. Scale bars: 10 µm. All retinas from mice aged P25.

4 Supplemental information for Fig. 4

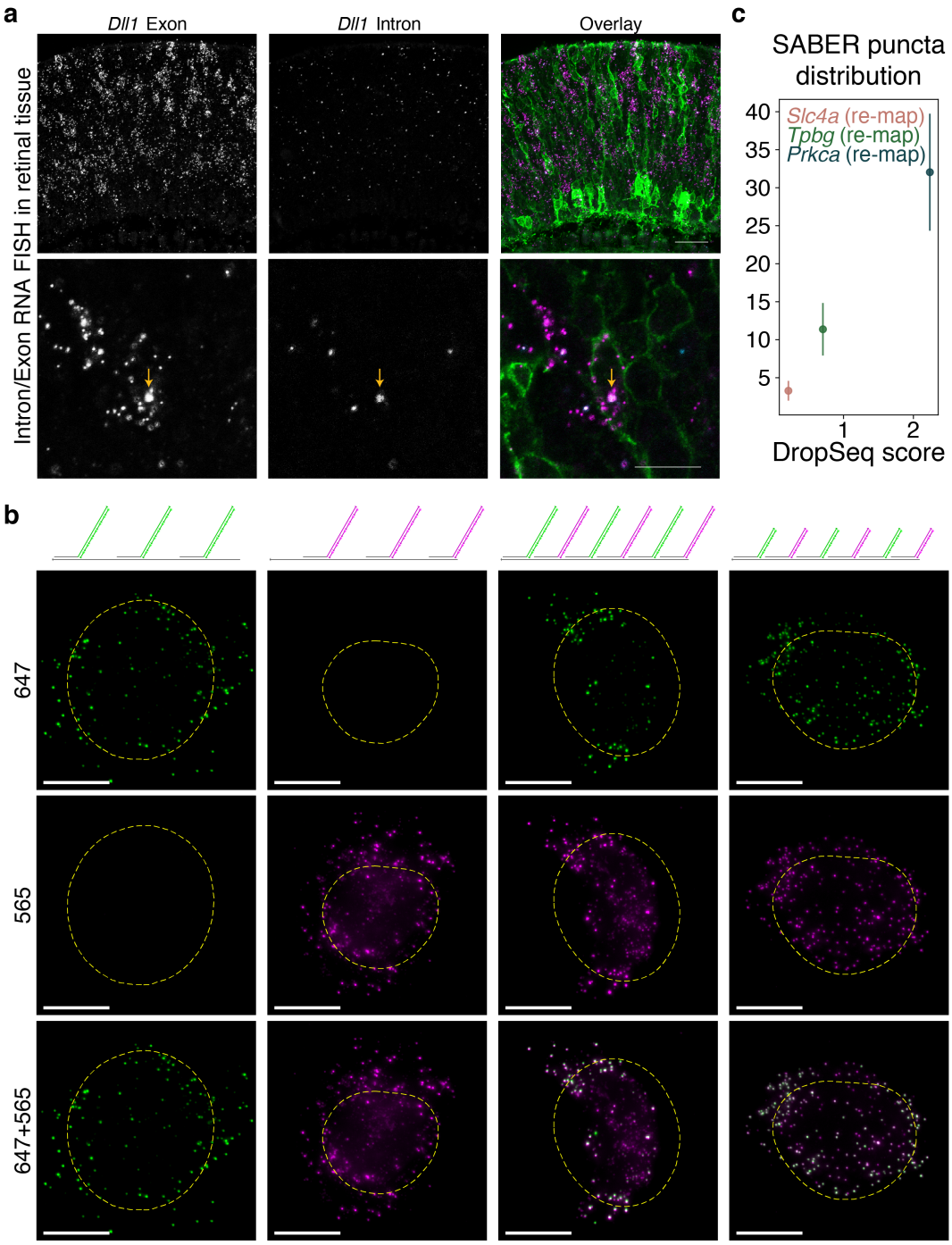

Supplementary Figure 6: **Intron/Exon SABER-FISH, control images for two-color colocalization, and puncta quantification for re-mapping.** **a**, Co-detection of intronic and exonic sequences. Bottom panel shows magnified view. Retinas were electroporated with CAG-mGFP, detected after *in situ* by IF for GFP, to visualize cell boundaries. Arrow indicates presumed site of transcription based on overlap of intronic and exonic sequence detection. **b**, Control conditions for Fig. 4d show no bleedthrough between the 565/647 detection channels. The longer concatemer condition showed reduced co-localization of puncta (67-82%) than the shorter extensions (92-95%) as determined by our automated segmentation pipeline, demonstrating the importance of length programmability of concatemers. See Supplemental Experimental Procedures for more information. **c**, Detection of transcripts using re-mapped probes for *Prkca* and *Tpbg*, along with *Slc4a* (Fig. 4e-f), compared against average number of transcripts per cell measured by Drop-Seq.[8] Means with standard deviations of SABER puncta per cell are shown. n(cells): n(*Slc4a*)=38; n(*Tpbg*)=45; n(*Prkca*)=52. Scale bars: 10 µm.

5 Supplemental information for Fig. 5

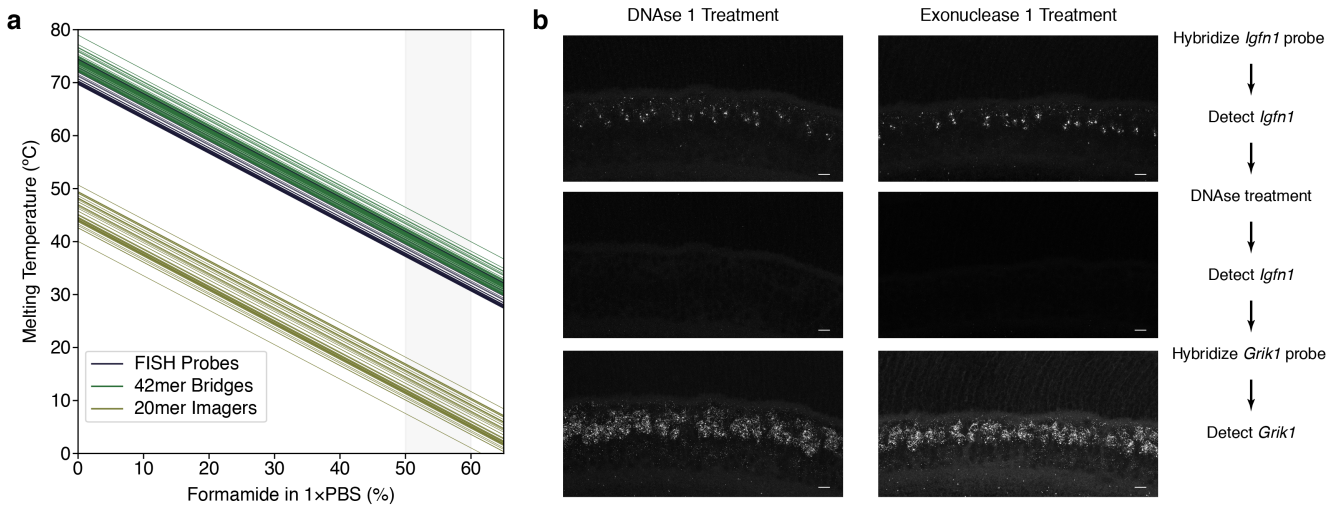

Supplementary Figure 7: **Melting temperature calculations for formamide-based exchange and data for DNase- and Exonuclease-based exchange. a**, Melting temperatures calculated using Biopython[3] for 20mer imager sequences, 42mer bridge sequences, and probes (corresponding to the sequences analyzed in Supplementary Fig. 1h-i were modeled under different formamide concentrations in 1×PBS. Typically, 50%-60% formamide in 1×PBS is effective in rapidly destabilizing imager strands while leaving underlying bridge and probe sequences hybridized. **b**, Sequential hybridization demonstrating recycling of concatemer sequences by digestion with DNase I or Exonuclease I. First, type 7 ON bipolar cells are detected by probing for the marker gene *Igfn1*.[8] After detection, DNases are applied and successful probe degradation is confirmed by reapplication of fluorescent imagers. Finally, a second round of probe hybridization is performed using a probe set bearing the same concatemer to detect a different bipolar cell population (OFF bipolar cells, *Grik1* transcript), to confirm stability of RNA for FISH detection after DNase treatment. Scale bars: 10 μm.

6 Four-color colocalization of *Cas9*

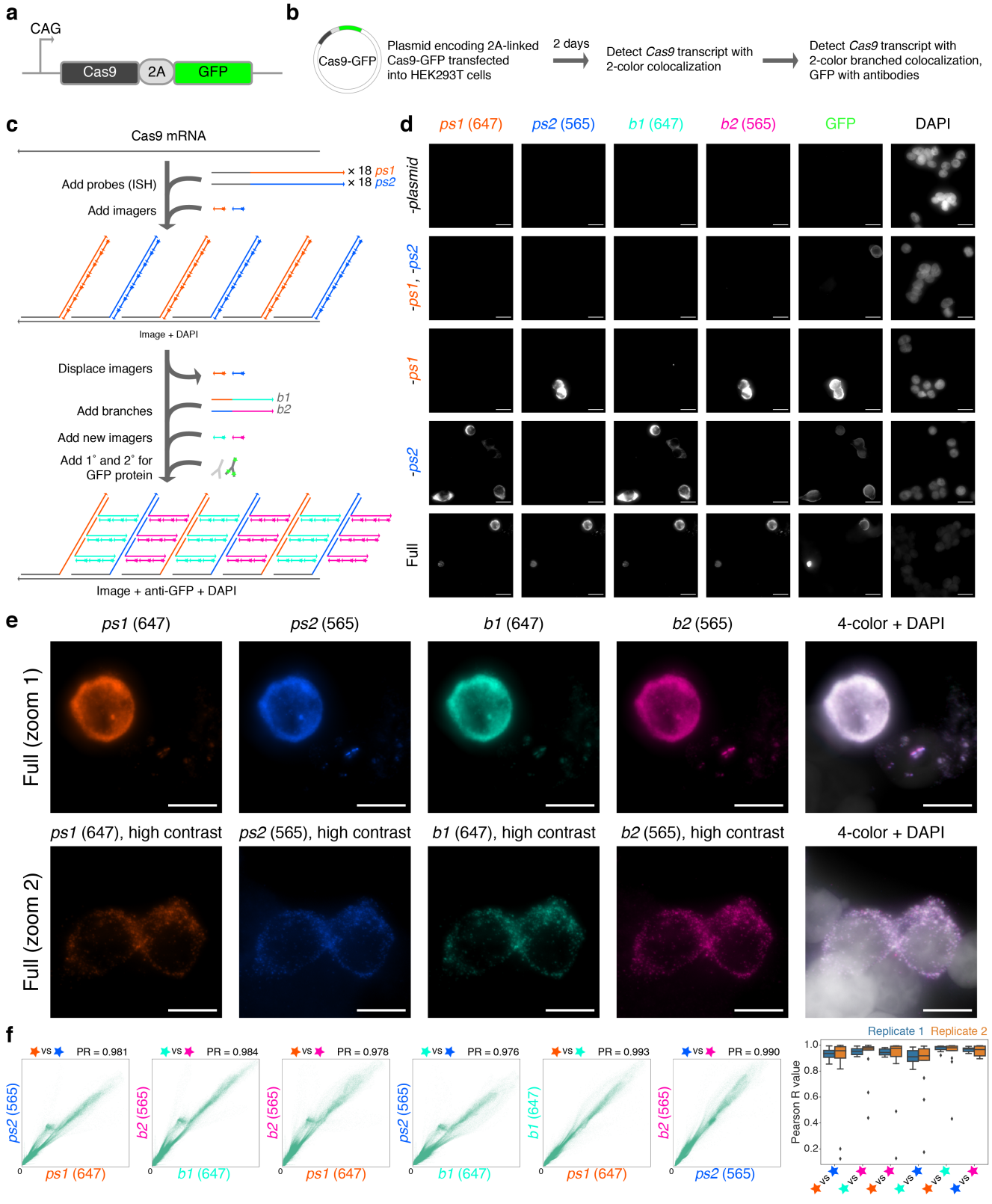

Supplementary Figure 8: ***Cas9* extended and branch signal colocalization experimental data and analysis. a**, Schematic of Cas9 and GFP genes linked together with a 2A peptide sequence. **b**, Workflow describing plasmid transfection and two rounds of SABER-FISH. **c**, Reaction schematics depicting an initial two-color colocalization (orange, blue) SABER-FISH experiment and imaging followed by fluorescent exchange and branching to two new sequences (cyan, magenta). Just before the second round of imaging the same regions, primary and secondary antibodies were incubated to visualize GFP (green). **d**, Matrix of images showing expected signal morphology in each channel for each of four controls alongside the primary four-color colocalization experiment (Full). We note that branch conditions were imaged with significantly lower exposure times. Scale bars are 20 μm. **e**, Higher magnification images and overlay of the four-color colocalization for a high expressing cell (top) and low expressing cells (bottom, higher contrast) show strong colocalization between all four channels. Scale bars are 10 μm. **f**, After DAPI-based alignment of images, Pearson R values between all pairs of channel pixel values (n(pixels) = 2048×2048 minus empty and saturated pixel values) in the image showed above (part **d**, bottom and part **e**, top) show strong cross-correlation between signal morphologies (0.98-0.99) (left). Values are highest for the conditions comparing between the same fluorescent channel, likely due to an absence of chromatic shift as there would be between the 647 and 565 channels. Box plot of Pearson R calculated for all regions imaged for two replicate chambers (right). Note that the outliers with low correlation were found to be images with very low signal (either untransfected cells or very low expression) and single-channel fluorescent clumps of unknown origin outside cell boundaries. Median line and quartiles shown, with points outside 1.5× the interquartile range shown as outliers. n(images): n(Replicate 1)=8; n(Replicate 2)=13.

7 Supplemental information for Fig. 6

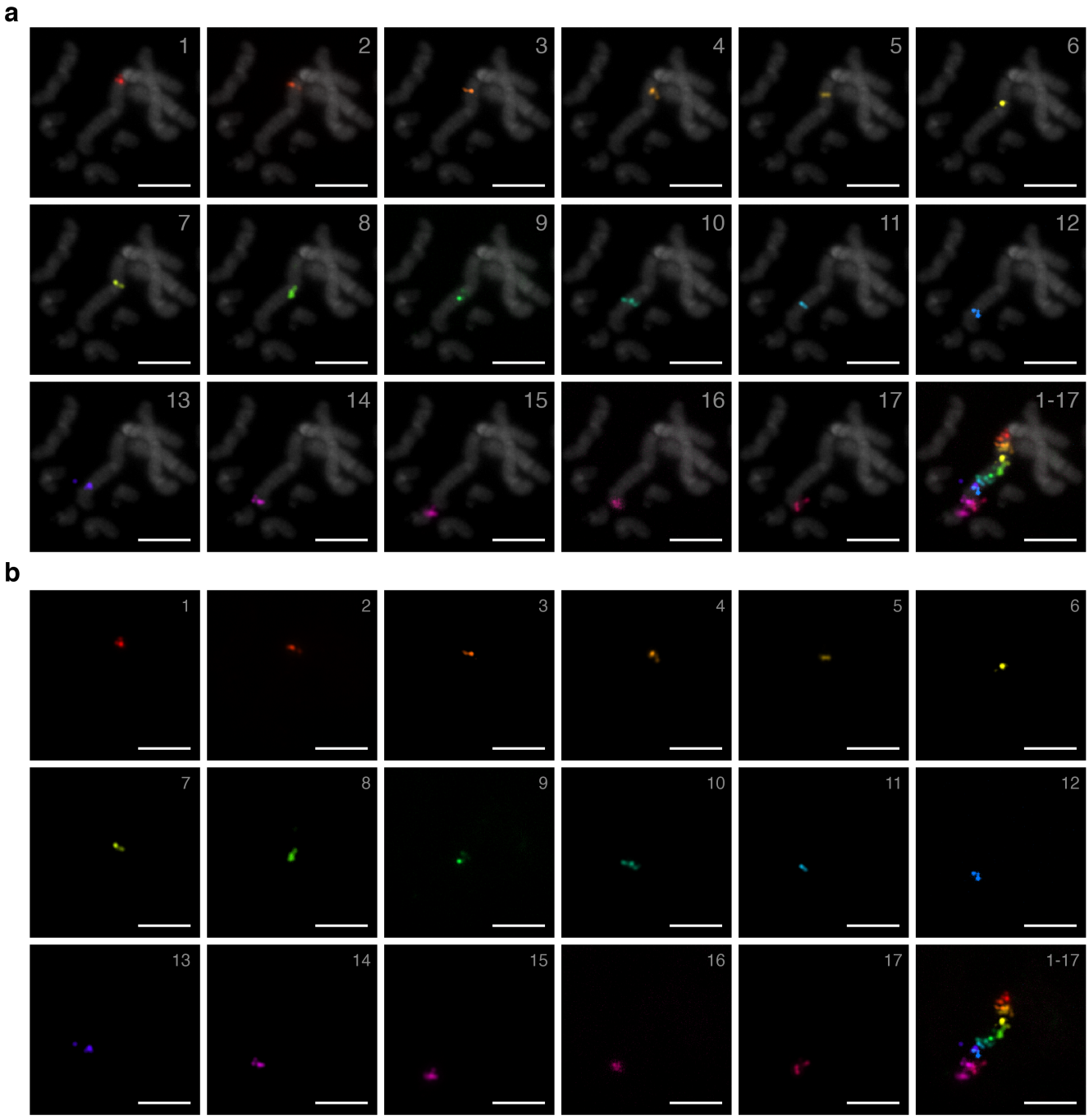

Supplementary Figure 9: **Single color channels for 17-color experiment.** **a**, Individual channel images overlaid on the DAPI channel corresponding to the experiment Fig. 6a-b, along with an overlay of all 17 positions, are shown. **b**, Individual channel images and 17-channel overlay corresponding to the experiment Fig. 6a-b. Scale bars: 5 μm.

8 Supplemental information for Fig. 7

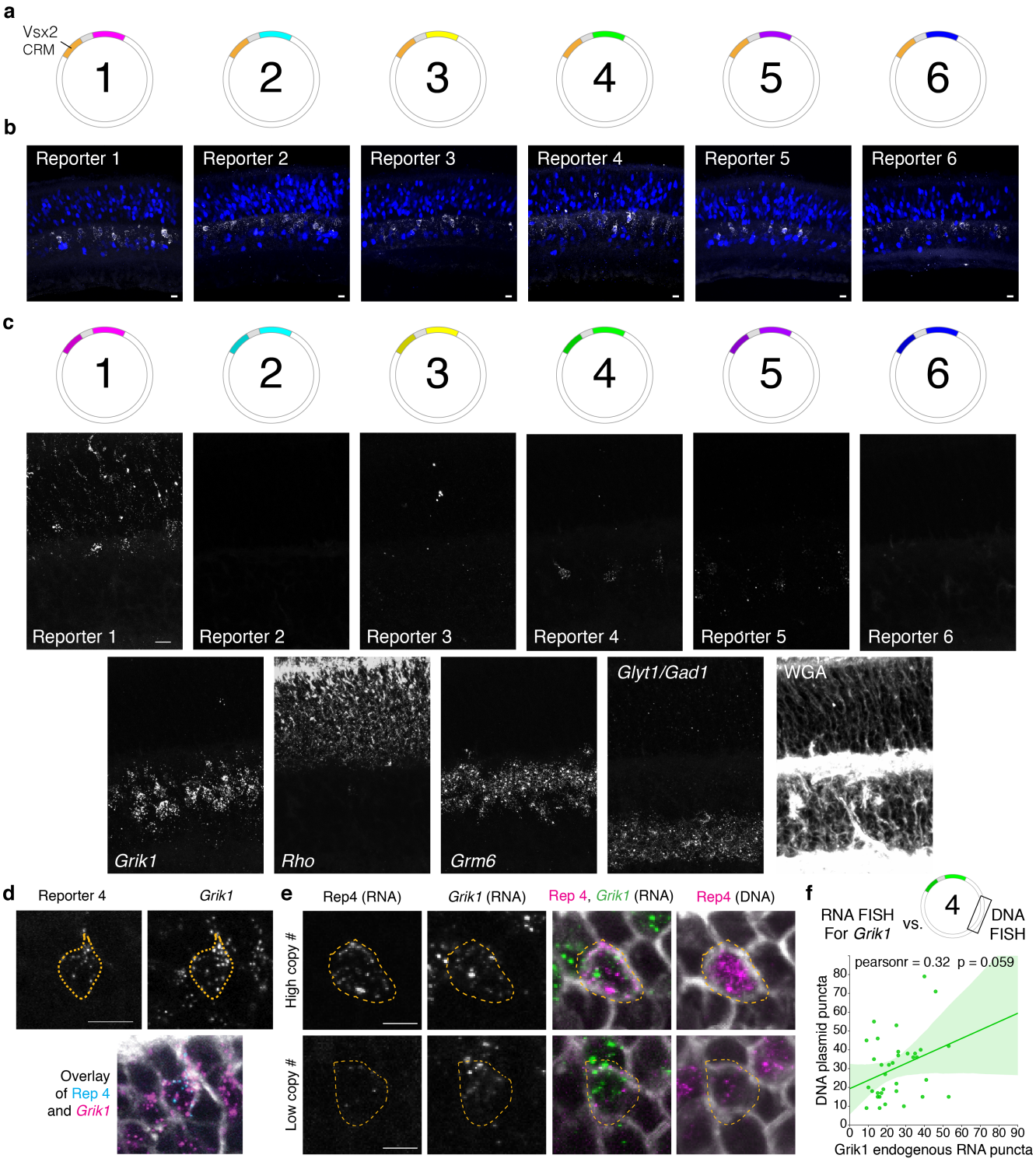

Supplementary Figure 10: **Reporter sequence validation and additional data for testing of candidate cis-regulatory modules (CRMs). a**, Plasmid design for reporter testing, wherein each reporter is inserted downstream of a common enhancer that drives expression in bipolar cells. **b**, Detection of each reporter RNA shows expression confined to the bipolar cell layer, consistent with the described activity of the *Vsx2* enhancer used. Shown in blue is a TagBFP co-electroporation marker for patch identification. Scale bars are 10 µm. **c**, All channels detected by spectral and serial multiplexing for the experiment described in Fig. 7. *Glyt1* and *Gad1* were detected with the same concatemer to label the amacrine population, composed of both glycinergic and gabaergic cells. Scale bar is 10 µm. **d**, Magnified image of a CRM-4/Reporter 4-expressing cell showing co-expression with *Grik1*. Scale bar is 10 µm. **e**, Magnified images for sequential RNA/DNA FISH prior to puncta detection, corresponding to Fig. 7j. Dashed outlines are manually drawn to highlight representative electroporated cells. Scale bar is 5 µm. **f**, Plot of plasmid copy number against *Grik1* expression shows no correlation, in contrast to the correlation observed for plasmid copy number and reporter expression (Fig. 7k). Pearson correlation coefficient (pearsonr) and p value shown. Shaded region indicates 95% confidence interval. n(cells)=35.

9 Additional supplementary materials

9.1 Sequences

Sequences for all experiments, along with those used to model orthogonality in Fig. 1 can be found in Supplementary Table 1.

9.2 Orthogonalities and melting temperatures

The cross-talk binding probabilities depicted in Fig. 1h-i and melting temperatures calculated under different formamide conditions for these probe, barcode, and primer (20mer imager, 30mer branch) sequences are listed in Supplementary Table 2.

9.3 PER reaction conditions

Panel-by-panel PER extension conditions can be found in the 'PER experiments' tab of Supplementary Table 3.

9.4 FISH incubation conditions

In situ hybridization (ISH), branch hybridization, and fluorescent hybridization condition details can be found in the 'FISH experiments' tab of Supplementary Table 3. Z depths of the max intensity projections displayed for tissue images are also listed.

9.5 Cell and puncta counts

Numbers of cells/tissues analyzed, puncta counts, and mean and standard deviations of puncta values for amplification fold enhancement experiments are reported in Supplementary Table 4.

9.6 User-friendly protocols

In the Supplemental Protocols file, we have provided a number of user-friendly protocols for designing and running PER concatemerization reactions *in vitro* and implementing SABER in cells and tissues.

10 Cost estimations

If material is prepared in bulk, each 100 µL PER solution can use about $0.265 in Bst polymerase (from McLab, BPL-300) polymerase, and unpurified hairpin with polyT tail costs ~$0.07 per reaction ($3.50 for ~5 mL of 5 µM, unpurified from IDT). A typical probe pool of ~50 unpurified probe oligos would cost ~$250 for (IDT plate), producing enough material (10 nmole yield) for 10 mL of 1 µM of each solution, or 500 mL of pooled solution, which comes out to $0.05 per 100 µL PER solution. The cost of oligos and polymerase for each 100 µL reaction of this type would therefore be about $0.265 + $0.07 + $0.05 = $0.39. Each 100 µL reaction typically yields ~10 µg, and 1 µg of extension is added per 120 µL ISH solution (experiment), which brings the cost to ~$0.04 per target per experiment. If PER extensions are column-purified, up to ~100 µg can be purified at once with a Zymo column (e.g. DNA Clean & Concentrator-100 kit, Zymo # D4030, ~$3.42 per column) adding an additional $0.03 per target per experiment. Thus, the minimum cost per target per experiment is about $0.10.

While we later discovered that these lower cost reaction conditions worked well for SABER, several earlier experiments shown in this work used more expensive conditions: purified hairpins (~50× more expensive than unpurified) Bst polymerase from NEB (#M0275L, up to 6× more expensive than McLab Bst), and MinElute PCR purification columns (~15× more expensive than Zymo-100 columns due to reduced column capacity of 5 µg). The cost of a 100 µL PER solution with these conditions would be estimated at $5.14. The maximum cost per target per experiment is therefore estimated to be around 17× higher, at $0.51. If extensions are column purified, this would add an additional $0.50 per target per experiment. This puts the maximum cost per target per experiment around $1 (for 120 µL ISH solution).

For microarray synthesis, the upfront cost of synthesis is substantially higher (~$3200-$5000 for an 18k library), although this provides enough base material for an essentially unlimited number of experiments after amplification. The experiments using array-synthesized oligos all utilized the modular bridge design strategy, so the cost of probe preparation can be added to the cost of the PER concatemerization. The cost of emulsion PCR and secondary PCR amplification per experiment is negligible (~$0.05), and most of the cost of probe preparation comes from the in vitro transcription (IVT) and reverse transcription (RT) processes. IVT is estimated to cost about $80 for a 240 µL reaction ($55 for NEB HiScribe, $17 for RNaseOUT, $7 for 2×Zymo-100 DNA Clean & Concentrator kits), and RT is estimated to cost about $70 for 240 µL (~$47 for Maxima H Minus RT enzyme, $17 for RNaseOUT, and $7 for 2 additional columns). This reaction typically produces enough material for ~100 reactions (using 500 nM probe in 120 µL ISH solution) for a total cost of about $150, so the additional cost added for these experiments is estimated to be approximately $1.50. Since libraries typically include probes for several targets (3-17 experimentally demonstrated), the cost per target per experiment would be further reduced to $1.50 / n for n targets.

Fluorescent imager oligos ordered on the 100 nmole synthesis scale from IDT, with typical 12 nmole yield, cost around $300 for 12 mL of 1 µM solution. This translates to about $3.00 per target per (120uL) fluorescent hybridization solution for 1 µM incubations and $0.60 for 0.2 µM, which also performed well. The cost would be further reduced if instead these oligos were ordered at larger synthesis scales or conjugated in bulk in-house. For example, we estimate the cost of conjugating 12 nmole of fluorescent oligos to be approximately 5× cheaper (~$65), based on ordering 250 nmole scale oligos unpurified from IDT with 3' amino modifiers, conjugating them to Cy3B-NHS dyes, and then purifying with a NAP-5 column. It is likely fluorescent imagers would work without further HPLC purification, but the cost this would add per experiment is also negligible. Also, while these parameters reflect conditions used for experiments in the paper, we note that lower concentrations of probe and imager oligos as well as fewer probes per target can also perform efficiently, particularly if paired with longer incubation times. This provides further opportunity for cost reduction.

11 Supplemental references

1. Kishi, J. Y., Schaus, T. E., Gopalkrishnan, N., Xuan, F. & Yin, P. Programmable autonomous synthesis of single-stranded DNA. *Nature Chemistry* (2017).
2. Beliveau, B. J. *et al.* OligoMiner provides a rapid, flexible environment for the design of genome-scale oligonucleotide in situ hybridization probes. *Proceedings of the National Academy of Sciences* (2018).
3. Cock, P. J. A. *et al.* Biopython: freely available Python tools for computational molecular biology and bioinformatics. *Bioinformatics* **25**, 1422–1423 (2009).
4. Dirks, R. M. & Pierce, N. A. A partition function algorithm for nucleic acid secondary structure including pseudoknots. *Journal of Computational Chemistry* **24**, 1664–1677 (2003).
5. Dirks, R. M. & Pierce, N. A. An algorithm for computing nucleic acid base-pairing probabilities including pseudoknots. *Journal of Computational Chemistry* **25**, 1295–1304 (2004).
6. Dirks, R. M., Bois, J. S., Schaeffer, J. M., Winfree, E. & Pierce, N. A. Thermodynamic Analysis of Interacting Nucleic Acid Strands. *SIAM Review* **49**, 65–88 (2007).
7. Carpenter, A. E. *et al.* CellProfiler: image analysis software for identifying and quantifying cell phenotypes. *Genome biology* **7**, R100 (2006).
8. Shekhar, K. *et al.* Comprehensive Classification of Retinal Bipolar Neurons by Single-Cell Transcriptomics. *Cell* **166**, 1308–1323.e30 (2016).
9. Schneider, C. A., Rasband, W. S. & Eliceiri, K. W. NIH Image to ImageJ : 25 years of image analysis HISTORICAL commentary NIH Image to ImageJ : 25 years of image analysis. *Nature Methods* **9**, 671–675 (2012).